Isotope Separation by Thermal Diffusion in Liquid Metal

Abstract. *Isotopic enrichment of several percent has been obtained in liquid lithium metal by applying a temperature gradient over a single-stage separation column. For other metals the method should have the highest efficiency, if these have low melting points and are liquids over a wide temperature range.*

As a result of our studies of atomic mobilities in liquid metals (*1*), we have developed a single-stage column for the separation of isotopes by thermal diffusion (thermotransport, thermomigration). A steel tube, 10 mm in inner diameter, was held in a vertical position. A bundle of stainless steel capillaries (50 mm long and 0.5 mm in inner diameter) was placed in the bottom portion of the tube (separation portion) in order to decrease convectional stirring. A lump of lithium metal was placed above the capillary bundle and the whole apparatus was evacuated. While still under vacuum, the metal was melted and poured into the separation portion of the tube, covering the orifices of the capillaries. A switch of a valve then caused the vacuum to be replaced by a slight surplus pressure of argon, ensuring break-free filling of the capillaries. The volume of Li metal was so chosen that the surface of the liquid was about 5 mm above the capillary bundle. The metal was kept under a temperature gradient (530°C at the surface, 250°C at the bottom end of the column) for 4 days to ensure the establishment of a steady state. Subsequent analysis showed an isotope separation of about 4 percent between the top and the bottom of the tube with the light isotope enriched at the high temperature.

Since the quantities which may be separated by this process approach 1 cm^3, this appears to be a relatively easy and inexpensive way to obtain isotopic enrichments of a few percent, even in a considerable bulk of material. According to the theory (*2*), the obtainable separation is proportional to the relative mass difference of the isotopes and to the factor $(T_c^{-1} - T_h^{-1})$, where T_c and T_h are, respectively, the temperatures at the coldest and hottest parts of the column. The process is thus especially applicable to metals with low melting points and those which are liquids over a wide temperature range.

AADU OTT*
Physics Department, Chalmers University of Technology, Gothenburg, Sweden

References and Notes

1. A. Ott and A. Lundén, *Z. Naturforsch.* **19a**, 822 (1964); A. Lodding and A. Ott, *ibid.* **21a**, 1344 (1966); A. Ott, L. Löwenberg, A. Lodding, *ibid.* **22a**, 2122 (1967).
2. A. Lodding, *ibid.* **21a**, 1348 (1966).
* Present address: Department of Physics, University of Arizona, Tucson 85721.

3 February 1969

Martian Craters: Comparison of Statistical Counts

Abstract. *Comparisons of the various crater counts obtained from the Mariner IV photographs indicate that, out of 300 to 600 possible craters mapped by different investigators, only about 120 craters can be reliably identified. Thus, only a lower limit for the Martian crater density can be established from the Mariner IV data.*

In an initial report on the Mariner IV results, Leighton *et al.* (*1*) indicated that over 70 craters were readily distinguishable on the unrefined photographs. In a subsequent analysis of the best of the preliminary photographs (frames 7 through 14) I counted 89 reasonably well-defined craters (*2*). This count was considered to be a lower limit for the number of craters and it was estimated that the loss of craters larger than 20 km in diameter, due to poor definition, amounted to less than 30 percent. Thus, the estimated upper limit for the number of craters visible on these frames was about 120. A similar result was obtained by Hartmann (*3*) who found 85 craters on the best photographs.

In apparently exhaustive studies of the crater density Chapman *et al.* (*4*), using frames 2 through 15 of the preliminary photographs, cataloged 288 craters; Marcus (*5*) counted 645 craters on frames 3 through 14. Similar results were obtained by Leighton *et al.* (*6*) who found at least 300 and possibly 600 craters on ACIC (Aeronautical Chart and Information Center) renditions of the final, calibrated, and contrast-enhanced pictures. Since the counts by Leighton *et al.* were not made directly from the photographic records, their results are open to question. Chapman *et al.*, Leighton *et al.*, and Marcus have assumed that the apparent consistency of their crater counts confirms their conclusions.

Table 1. Commonality of crater counts on frames 4, 7, and 11.

Crater class	Craters listed (*4*) (No.)	Common craters (av. %)
	Frame 4	
A	2	75
B	8	25
C	9	0
	Frame 7	
A	19	68
B	20	18
C	6	0
	Frame 11	
A	14	100
B	9	33
C	9	45

In view of the low contrast and generally poor definition of the pictures, the identification of 300 or more craters seems questionable. Since no direct comparison of the individual craters was made, the apparent confirmation of the results could be fortuitous. Fortunately, a limited comparison can be made, since line drawings of the craters counted in frames 4, 7, and 11 are given by Chapman *et al.* and the ACIC renditions for all frames are given by Leighton *et al.* (*6*).

For purposes of this study, each line drawing was rectified photographically by projecting a negative image of the drawing onto a plane which was inclined so that the borders of the drawing exactly matched the borders of the corresponding ACIC map (the borders of each version correspond to the edges of the original frames). Sheet film was then placed on the plane so that the resulting film positive could be used as an overlay.

The comparisons of the two interpretations of frames 4, 7, and 11 were made by superimposing each transparency on the corresponding ACIC map and determining which craters were common to both. In order to allow for minor cartographic errors, several different fits of the pairs of transparency maps were tried. The numerical results (Table 1) represent an average of several different attempts to correlate the craters of each frame. Figures 1 through 3 show the ACIC maps of frames 4, 7, and 11 with the transparencies superimposed in positions representing the best fits between the two renditions.

A crater was considered to be com-

mon to both interpretations if its diameters did not differ by more than about 25 percent and its position did not vary by more than about one-half of its radius between the overlap and the ACIC map. These criteria are thought to be commensurate with the quality of the Mariner IV pictures and they also allow for the rejection of fictitious craters which were defined out of preconception and random curvilinear markings at the limit of detectability.

An indication of the difficulty associated with working with the Mariner IV records and of the possible influence of preconception can be seen in Figs. 1 through 3. By analogy with the lunar craters, it is expected that the Martian craters are all generally circular (or polygonal) in shape. Inasmuch as the photographs that Chapman *et al.* worked with were unrectified, the craters would appear elliptical in most of the frames. The fact that, upon rectification, the line drawings (especially for frame 4, that is, Fig. 1) do not generally show circular outlines indicates that the degree and direction of the foreshortening were incorrectly estimated; thus the elliptical shapes, looked for and found, do not in fact generally correspond to craters. Such fictitious craters result from the ability of observers to define geometric shapes out of a matrix of random markings. This type of error would most seriously affect the results obtained from frames 2 to 6 and probably frames 13 to 15, especially for the larger craters.

Chapman *et al.* have divided the craters they defined into three classes. Class A contains those features which are definitely craters; class B contains features which definitely occur on the Martian surface and are probably

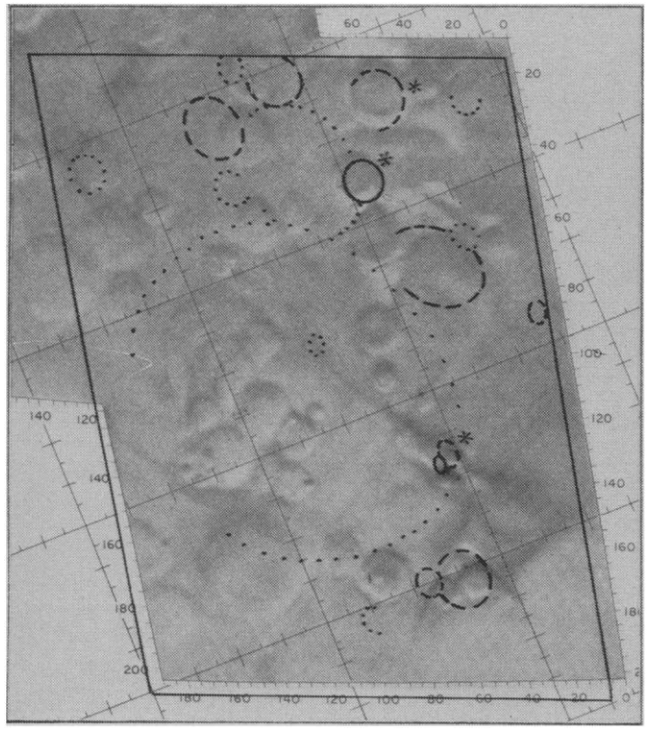

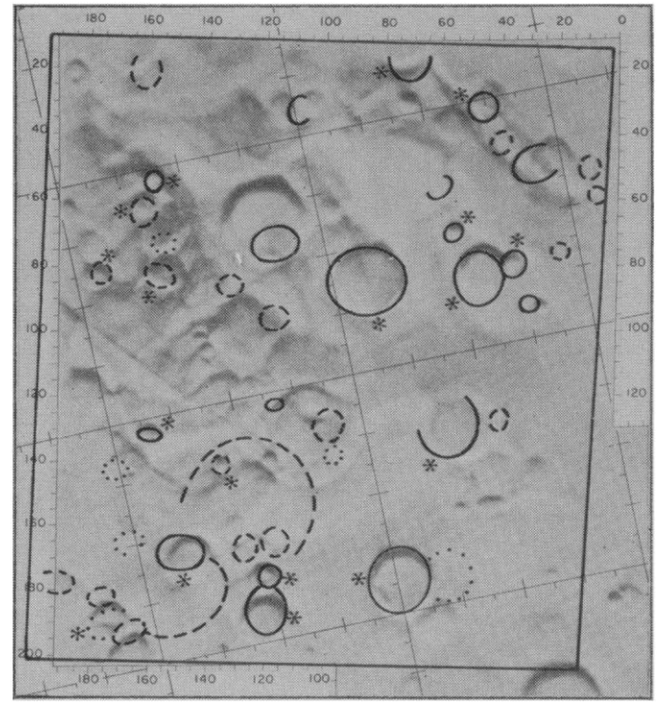

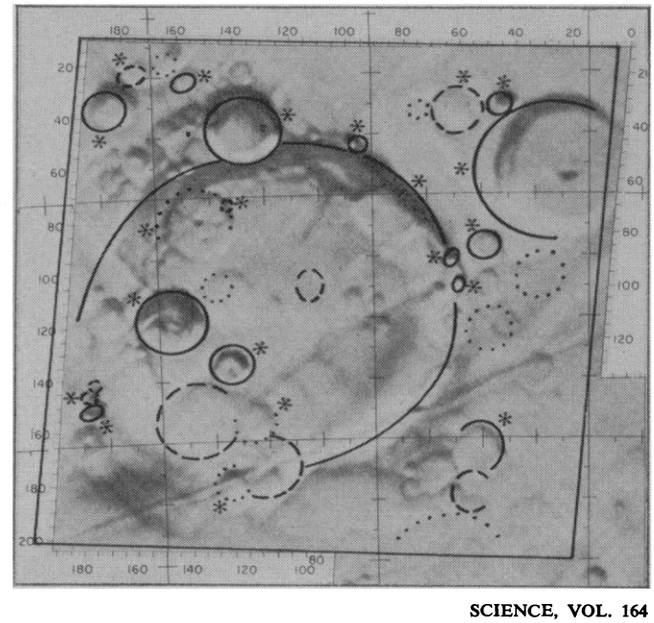

Fig. 1 (above left). Comparison of two interpretations of frame 4 of the Mariner IV photographs. The two versions are slightly misaligned in order to show the most favorable coincidence of craters. Craters of class A are indicated by solid lines, those of class B by dashed lines, and those of class C by dotted lines. Those craters shown in the rectified line drawing which are considered to be common to both interpretations are marked by an asterisk.

Fig. 2 (above right). Comparison of two interpretations of frame 7 of the Mariner IV photographs.

Fig. 3 (right). Comparison of two interpretations of frame 11 of the Mariner IV photographs.

craters; and class C contains objects which may be craters. These classes have been retained in this analysis.

Table 1 gives the percentage of craters in each class in frames 4, 7, and 11 which are common to both interpretations. The results given are the averages of several different overlap fits; the spread of the data is 10 percent for frames 7 and 11 and 25 percent for frame 4. If it is assumed that the crater commonality factors obtained for frames 4, 7, and 11 can be applied to the other frames and if we allow for the differences in the quality of the different frames, then, out of the nearly 300 craters mapped by Chapman *et al.* and the 600 mapped by Leighton *et al.* (*6*), there are only 115 to 120 common to both counts. If only frames 7 through 14 are considered, then there are about 100 craters common to both interpretations, a value which is consistent with the results obtained by Binder (*2*) and Hartmann (*3*). The comparisons also show that only 75 to 80 percent of the craters of class A, 30 percent of those in class B, and less than 10 percent of those in class C mapped by Chapman *et al.* represent real craters.

It seems that the *observed* crater density derived earlier (*2*, *3*) is essentially correct and therefore that the *observed* Martian crater density is below that of the lunar uplands by a factor of nearly 2. I would emphasize that the *actual* crater density may very well be greater than the *observed* crater density, but the evidence supporting large crater densities based on the Mariner IV photographs is questionable. The Mariner IV photographs are extremely important because they have shown the presence of a large number of craters on the surface of Mars. However, an accurate evaluation of the crater density must await improved definition.

ALAN B. BINDER
Illinois Institute of Technology Research Institute, Chicago 60616

References and Notes

1. R. B. Leighton, B. C. Murray, R. P. Sharp, J. D. Allen, R. K. Sloan, *Science* **149**, 627 (1965).
2. A. B. Binder, *ibid.* **152**, 1053 (1966).
3. W. K. Hartmann, *Icarus* **5**, 565 (1966).
4. C. R. Chapman, J. B. Pollack, C. Sagan, *Smithsonian Astrophys. Spec. Rep. 268* (1968).
5. A. H. Marcus, *Science* **160**, 1333 (1968).
6. R. B. Leighton, B. C. Murray, R. P. Sharp, J. D. Allen, R. K. Sloan. *Jet Propulsion Lab. Tech. Rep. 32–884* (California Institute of Technology, Pasadena, 1967).

30 December 1968

Podocarpus from the Eocene of North America

Abstract. *A few leafy gymnosperm shoots were found in Eocene deposits of southeastern North America. Similar fossil material from Tertiary deposits in North America has been identified as* Taxodium, Taxites, *and* Sequoia. *This new fossil material is not related to these genera but belongs to* Podocarpus *section* Stachycarpus. *This is the first fossil record of this section in North America.*

Eocene floras have been described from western Tennessee (*1*). New collections from this area have yielded gymnospermous fossils, including compressions (Fig. 1, A and B) and a whole "mummified" shoot (Fig. 1C). Some cuticular material is preserved in nearly all of the leaves.

The shoots have stout stems with spirally arranged leaves that are disposed distichously. The leaves are needle-shaped, narrowed at the base, petiolate, and have an obtuse apex. They are unequally amphistomatic (having stomata on both surfaces) (Fig. 1D); the stomata are confined to a single row on either side of the midrib and are oriented parallel to the long axis of the leaf. There are conspicuous thickened rings of cutin (Fig. 1, E and F) overlaying the accessory cells and surrounding the stomata. Thickened rings of cutin have been observed surrounding stomates in the genus *Podocarpus* (*2*).

Podocarpus has been subdivided into several sections (*3*). The species of *Podocarpus* belonging to the section *Stachycarpus* have small yewlike spirally arranged leaves that are disposed distichously (*4*). A comparison of gross morphology and fine features of the fossil cuticle to those of the cuticle of modern species in this section confirm this fossil material as *Podocarpus* section *Stachycarpus* (*5*).

Florin (*6*) described some poorly preserved material from Eocene deposits in Chile which he provisionally placed in the section *Stachycarpus*. In another paper (*7*) he mentioned, but did not describe, some fossil material which he regarded as *Podocarpus* section *Stachycarpus*. Some early Tertiary (probably Eocene) fossil material from Tasmania has been identified as *Podocarpus* section *Stachycarpus* subsection *Idioblastus* (*8*). This subsection includes modern species now living in New Caledonia and Queensland in Australia which have idioblastic sclerids (*9*). The fossil material described in this paper, two modern New Zealand species (*Podocarpus spicatus* and *P. ferrugineus*), and all the modern American species of the section *Stachycarpus* are included in the subsection *Euprumnopitys*.

There have been no previous reports of leafy shoots of *Podocarpus*, section *Stachycarpus*, from the fossil record of North America. Previously, similar gymnosperm material with spirally arranged leaves from Tertiary deposits in North America has been identified as *Taxodium, Taxites,* and *Sequoia* (*1, 10*). *Metasequoia* is not generally confused with these genera because of its subopposite leaf arrangement. On the basis of gross morphology alone, this fossil material can not easily be distinguished from *Taxodium, Taxites* (*Taxus*), and *Sequoia.* However there are unique features of the cuticle which identify it as *Podocarpus*. The stomata of *Taxodium* are oriented in a random fashion on the lower surface of the leaves; those of *Taxus, Sequoia,* and *Podocarpus* are oriented parallel to the long axis of the leaves. The epidermal cells and accessory cells of *Taxus* are conspicuously papillate; those of *Podocarpus* are not. Thickened rings of cuticle are lacking in *Sequoia;* they are prominent in this fossil material and to some extent in *Podocarpus*. Because the leafy shoots of these genera cannot easily be differentiated when they lack cone material, the use of cuticular analysis is essential to the identification of fragmentary fossil leafy shoots. Until the fine features of the cuticle were carefully compared the material described in this paper was thought to belong to the genus *Sequoia* (*11*). Thus it is very possible that the reason no previous reports of fossils of *Podocarpus* section *Stachycarpus* have been made in North America is that identifications of leafy shoots of gymnospermous material have been made on the basis of gross morphology alone and this genus and section has not been considered when identifications have been made.

There are several reports of *Podocarpus* pollen from Mesozoic sediments of North America (*12*) and one report of *Podocarpus* wood from Eocene sediments in Washington (*13*). The pollen record of *Podocarpus* is believed not to extend into Tertiary sediments of North America (*14*). However, there is some indication from the pollen rec-